

Investigation on the adsorption mechanism of copper (II) ions onto a biosorbent based on lemon balm

L. P. Ivanova, P. S. Vassileva, V. G. Koleva, A. K. Detcheva*

Institute of General and Inorganic Chemistry, Bulgarian Academy of Sciences, Acad. Georgi Bonchev Str., Bl. 11, 1113, Sofia, Bulgaria

Received: August 17, 2022; Revised: February 25, 2023

In the present work an attempt is made to elucidate the mechanism of Cu(II) adsorption on a plant material based on lemon balm. Batch experiments were carried out in order to study the effects of acidity, contact time and initial metal concentration on Cu(II) removal. Langmuir, Freundlich and Dubinin-Radushkevich isotherm models were used to explain equilibrium experimental data and the maximum adsorption capacity was calculated. The mechanism of retention of copper ions on the biosorbent surface was studied by means of SEM, FTIR and XPS methods, as well as low-temperature nitrogen adsorption. Desorption experiments were also performed. It was proved that the investigated plant material could be used for the removal of copper ions from contaminated waters.

Keywords: Lemon balm, biosorption, copper ions, SEM, FTIR, XPS

INTRODUCTION

Heavy metal pollution is one of the most important problems around the world nowadays due to their toxic effects and persistence [1]. Copper is among the most common contaminants, found in surface water and groundwater, as well as industrial wastewater [2]. Copper pollution is generated from various sources and has resulted in an accumulation of large quantities of liquid effluents, loaded with high levels of toxic metallic species. It is of great importance to remove or reduce the concentration of copper ions before their discharge into aquatic environments, because it is harmful for living beings, especially for water organisms. Conventional treatment techniques like chemical precipitation, activated carbon adsorption, reverse osmosis, ion-exchange, membrane processes, ultrafiltration, solvent extraction, electrochemical processes, etc, used for removal of metal ions from aqueous solutions, have disadvantages and biosorption can be a reliable low-cost and eco-friendly alternative of these methods [3, 4]. The mechanism of this process relies on sorption of metal ions from aqueous solution to chemical functional groups present on the surface of the cell wall of the biomass [5]. It is known that lignocellulosic materials have good sorptive characteristics due to their structure. A number of studies discuss the use of biosorbents for heavy metal removal, but there is a growing interest in utilizing biosorbents, based on ethereal oil plants [6, 7].

Lemon balm (*Melissa officinalis* L.) as a representative of the ethereal oil plants is a perennial herbaceous plant in the mint family, native to

South-Central Europe, the Mediterranean Basin, Iran, and Central Asia, but now naturalized elsewhere. Different parts of the plant are used in folk medicine for their digestive, carminative, antispasmodic, sedative, analgesic, tonic, and diuretic properties. Various studies have shown that it also possesses high antioxidant activity through its chemical compounds including high amount of flavonoids, rosmarinic acid, gallic acid, phenolic contents [8]. Lemon balm, like other herbs, has multicomponent composition, a large part of which comprises cellulose, hemicellulose, pectin and lignin [6, 7]. Materials derived from lemon balm biomass are not used as biosorbents for metal ions until now, but they were used for remediation of polluted soils [9, 10].

In the present work a plant material based on *Melissa officinalis* L., denoted as MO was examined as a biosorbent for copper(II) ions. An attempt for elucidation of the adsorption mechanism using FTIR and XPS methods, as well as linear isotherm models has also been performed [11-13]. Desorption studies were carried out to estimate the possibility of regeneration of the used biosorbent.

EXPERIMENTAL

Materials and methods

The commercially available leaves of lemon balm were washed several times with distilled water to remove surface-adhered and water-soluble particles and dried at 60°C in an electric oven for 48 h. Thus prepared material was milled in an electric grinder to a size of particles below 200 µm. No other physical or chemical treatment was performed.

* To whom all correspondence should be sent:

E-mail: albena@svr.igic.bas.bg

The surface morphology of the biomaterial was observed on a scanning electron microscope (SEM) - Tescan instrument model SEM/FIB Lyra I XMU. The porous structure of the studied materials was investigated by low-temperature (−196°C) nitrogen adsorption using a Quantachrome Nova 1200 apparatus (Quantachrome Instruments, USA). Before nitrogen adsorption, the samples were degassed at 80°C for 3 h. Specific surface area was calculated on the basis of the Brunauer–Emmett–Teller (BET) equation; the pore size distribution was calculated according to the Barrett-Joyner-Halenda (BJH) method. The total pore volume was estimated in accordance with the rule of Gurvich at a relative pressure of 0.99. The volume of the micropores was calculated using the Dubinin-Radushkevich equation and the volume of the mesopores by the difference of $V_{total} - V_{micro}$. The Fourier transform-infrared (FTIR) spectra of the samples (raw MO and MO after Cu(II) sorption - MOS) were taken with a Nicolet spectrometer in the region of 4000–400 cm^{-1} using KBr pellets (resolution 2 cm^{-1} , 64 scans). Prior to the spectra measurements, the samples were pre-heated in a vacuum dryer at 120°C for 48 hours in order to eliminate partly the adsorbed water molecules. For each sample at least two KBr pellets were measured. XPS investigations were carried out by means of ESCALAB MKII spectrometer with Al K α (unmonochromatized) source at 1486.6 eV with a total instrumental resolution of ~1 eV, under a base pressure of 10^{-8} mbar. The C1s, O1s, N1s and Cu2p photoelectron lines were recorded and calibrated to the C1s line at 285.0 eV. XPSPEAK 4.0 fitting program was used for deconvolution of the photoelectron peaks. All data were recorded at 45° take-off angle.

Adsorption studies

Batch experiments were performed to determine the adsorption properties of the studied material. They were carried out using stoppered 50-mL Erlenmeyer flasks containing about 0.2 g of sample and 20 mL of aqueous solution of Cu(II) ions. The mixture was shaken at room temperature (20°C) by an automatic shaker. After the experiment the biomaterial was removed by filtration through a Millipore filter (0.2 μm). The initial and equilibrium copper concentrations were determined on a Prodigy 7 ICP-OES spectrometer (Teledyne Leeman Labs,

USA) and determinations were performed by the interference-free Cu-analytical line of 217.894 nm.

The amount of adsorbed copper ions per gram sorbent Q_e was calculated using the following relationship:

$$Q_e = (C_0 - C_e) * V/m \quad (1)$$

where C_0 = initial concentration ($mg L^{-1}$), C_e = equilibrium concentration ($mg L^{-1}$), m = mass of adsorbent (g), and V = solution volume (L). All measurements were replicated and the average results were discussed.

The effect of contact time on the amount of adsorbed Cu^{2+} ions with concentrations of 200 $mg L^{-1}$ was studied at pH 4.0. The effect of the medium acidity on Cu^{2+} removal efficiency was investigated over the pH range 1.8–5.0 with concentration of 200 $mg L^{-1}$ (pH-meter model pH 211, Hanna instruments, Germany). To determine the effect of the initial metal ion concentration on the adsorption capacity, Cu^{2+} concentrations in the range of 50–500 $mg L^{-1}$ at pH 4.0 were chosen. The initial pH of the working standard solutions was adjusted to the required value with 0.1 M HCl and NaOH solutions before mixing the suspension.

Desorption of copper from MO sorbent was studied in a batch system using three eluents: 0.1 M HNO_3 , 1 M HNO_3 and 0.1 M EDTA. Pre-adsorbed MO (0.1 g) was added to 10 mL of the above mentioned eluents and stirred for 24 h. The eluents were then filtered and tested for desorbed copper.

Working standard solutions of Cu^{2+} ions with concentrations of 50–500 $mg L^{-1}$ were prepared by stepwise dilution of a stock solution with concentration of 1000 $mg Cu L^{-1}$ ($CuCl_2$ in H_2O), Titrisol® Merck, (Darmstadt, Germany). All reagents used throughout the experiments were of analytical grade.

RESULTS AND DISCUSSION

Texture parameters

The calculated textural parameters of MO are summarized in Table 1. The studied material shows relatively low surface area and total pore volume. The calculated average pore diameter (6.4 nm) corresponds to a mesoporous structure. The measurement of slurry pH indicates that the sample displays pH values of 5.8, which points to slightly acidic reaction of the aqueous suspension.

Table 1. Texture characteristics and pH of the water leachates of MO

BET surface area, $m^2 g^{-1}$	Pore volume, $cm^3 g^{-1}$	Micropore volume, $cm^3 g^{-1}$	Mesopore volume, $cm^3 g^{-1}$	Average pore diameter, nm	pH
0.8	0.001	-	0.001	6.4	5.8

Effect of acidity and contact time

In the present study the removal of copper ions strongly depends on the acidity of the initial solutions. Upon increasing the pH values the amounts of adsorbed ions increased and the optimum pH range was found to be about 4.0 (Fig. 1a).

The adsorbed amount of Cu(II) ions increased rapidly within the first 2 min and remained constant after 10 min, thus indicating that the kinetics is fast and the equilibrium is reached (Fig. 1b). This is a proof for the good affinity of MO towards Cu(II) ions.

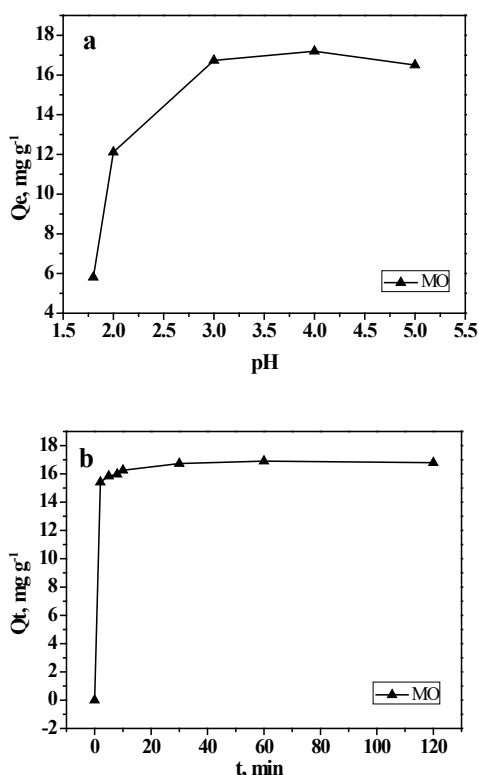


Fig. 1. Effect of acidity (a) and contact time (b) on the amount of adsorbed Cu(II) ions.

Adsorption isotherms

The effect of the initial copper ion concentration on the adsorption capacity was determined using Cu(II) concentrations in the range of 50-500 mg L⁻¹ at pH 4.0 (Fig. 2) and three isotherm models were employed to analyze the batch experimental data - the Langmuir, Freundlich and Dubinin-Radushkevich [7].

The linear form of the Langmuir isotherm is expressed by the following equation:

$$C_e/Q_e = 1/K_L Q_0 + C_e/Q_0 \quad (2)$$

where C_e is the concentration of metal ions in the equilibrium solution (mg L⁻¹), Q_e is the amount of ion adsorbed (mg) per unit mass of adsorbent (g), Q₀, the maximum adsorption capacity (mg g⁻¹), K_L is the Langmuir constant related to the enthalpy of the process.

The Langmuir model supports the following hypothesis: the adsorbent has a uniform surface; absence of interactions between the solid molecules; the sorption process takes place in a monolayer.

The linear form of the Freundlich model is expressed by the following equation:

$$\ln Q_e = \ln k_F + (1/n) \ln C_e \quad (3)$$

where k_F is a constant related to the adsorption capacity and n is an empirical parameter related to the intensity of adsorption.

The Freundlich model is valid for heterogeneous surfaces and predicts an increase in the concentration of the ionic species adsorbed onto the surface of the solid when increasing the concentration of certain species in the liquid phase.

The Dubinin-Radushkevich isotherm reveals the adsorption mechanism based on the potential theory. The linear form of the Dubinin-Radushkevich isotherm is described by the following equation:

$$\ln Q_e = \ln Q_m - \beta \varepsilon^2 \quad (4)$$

where Q_e is the amount of metal ion (mg) adsorbed per unit mass of adsorbent (g), Q_m is the maximum adsorption capacity (mg g⁻¹), β is the adsorption energy constant (mol² J⁻²), and ε is the Polanyi potential, described as:

$$\varepsilon = RT \ln(1+1/C_e) \quad (5)$$

where R is the gas constant (J mol⁻¹K⁻¹) and T is the temperature (K). The mean adsorption energy E (kJ mol⁻¹) can be calculated using the parameter β as follows:

$$E = 1/(-2\beta)^{1/2} \quad (6)$$

This is a substantial step to predict the mechanism of adsorption. Langmuir, Freundlich and Dubinin-Radushkevich equations are based on entirely different principles and the fact that the experimental results fit to one or other equation indicates the most probable adsorption mechanism.

Table 2. Constants of Langmuir, Freundlich and Dubinin-Radushkevich isotherms for the adsorption of Cu(II) ions onto the biomaterial MO

Langmuir parameters			Freundlich parameters			Dubinin-Radushkevich parameters		
Q ₀ (mg g ⁻¹)	K ₁ (L mg ⁻¹)	r ²	k _F (mg ¹⁻ⁿ L ⁿ g ⁻¹)	n (L mg ⁻¹)	r ²	Q _{m(0)} (mg g ⁻¹)	E (kJ mol ⁻¹)	r ²
59.95	0.031	0.9709	1.08	1.58	0.9525	27.42	0.146	0.7970

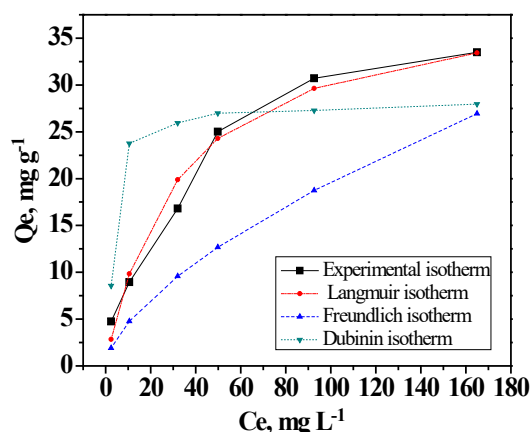


Fig. 2. Adsorption isotherms towards Cu(II) ions

It is important to note that every model has its own limitations in accurately describing equilibrium data. The corresponding parameters are given in Table 2. The correlation coefficients (r^2) showed that Langmuir model most adequately describes the adsorption process. This means that the surface of the investigated biomaterial is homogeneous, there are no interactions between the adsorbed molecules and the uptake of copper ions occurs by monolayer adsorption. The calculated values for non-linear chi-square test χ^2 , calculated as it is described by Gentsheva *et al.* [14] (0.0051, 0.3074 and 0.0362 for Langmuir, Freundlich and Dubinin-Radushkevich equations, respectively) confirm this assumption. The smaller the value of χ^2 , the better the experimental data with the given model are described.

The non-linear dependences of the amount of adsorbed Cu(II) ions from the equilibrium concentration using Langmuir, Freundlich and Dubinin-Radushkevich models and experimental data are given in Fig. 2. The constant k_F is an approximate indicator of adsorption capacity, while $1/n$ is a function of the strength of adsorption in the adsorption process. $1/n$ is a heterogeneity parameter, the smaller $1/n$, the greater is the expected heterogeneity [15]. If n is between one and ten, this indicates a favorable sorption process [16]. From the data in Table 2, the value of $n=1.58$ indicates that the

adsorption of Cu(II) onto MO is favorable. On the other hand, the linear Langmuir model is usually applied for calculation of maximum adsorption capacity. In the present study the maximum adsorption capacity for copper ions was found to be 59.95 mg g⁻¹. The adsorption capacity of lemon balm is compared with those reported in literature [7, 11, 17-23] (Table 3). It is evident that the biomaterial MO displays reasonably good adsorption capacity for Cu(II) and it could be used as potential adsorbent for the effective removal of these ions from contaminated aqueous solutions.

Table 3. Comparison of adsorption capacities with respect to Cu(II) ions in the present study with those reported in the literature.

Biosorbent	Q _{max} (mg g ⁻¹)	References
Watermelon rind	5.73	Liu <i>et al.</i> [17]
Banana peels	8.24	Liu <i>et al.</i> [17]
Sugarcane bagasse	9.48	Liu <i>et al.</i> [17]
<i>Lagenaria vulgaris</i> shell	12.15	Stanković <i>et al.</i> [18]
Chestnut shell	12.56	Yao <i>et al.</i> [19]
Persimmon leaves	19.42	Lee and Choi [20]
<i>Eichhornia crassipes</i>	22.70	Zheng <i>et al.</i> [11]
<i>Achillea millefolium</i> L.	28.11	Vassileva <i>et al.</i> [7]
<i>Thymus vulgaris</i> L.	38.93	Ivanova <i>et al.</i> [21]
Banana leaves	48.7	Darweesh <i>et al.</i> [22]
<i>Ocimum bacilicum</i> seeds	73.10	Adeel <i>et al.</i> [23]
<i>Melissa officinalis</i> L.	59.95	present study

Furthermore, desorption studies have also been performed. The Cu(II) ions adsorbed onto the

investigated biosorbent were eluted with 0.1M HNO₃, 1M HNO₃ and 0.1M EDTA. Dilute HNO₃ could not be used for desorption of Cu(II) ions (34% desorption). Both eluting agents 1M HNO₃ and 0.1M EDTA showed higher, equal recovery efficiency of 100%.

SEM analysis

The morphology and structure of the biosorbent MO before and after Cu(II) adsorption was investigated with SEM (Fig. 3). The SEM micrographs show that the investigated biomaterial is of rough and heterogeneous morphology, containing a large number of pores of different size. This type surface is expected to favor the sorption of various ions in the different parts of the biosorbent. As can be seen, the adsorbed copper ions (marked in green) are distributed homogeneously on the biosorbent surface.

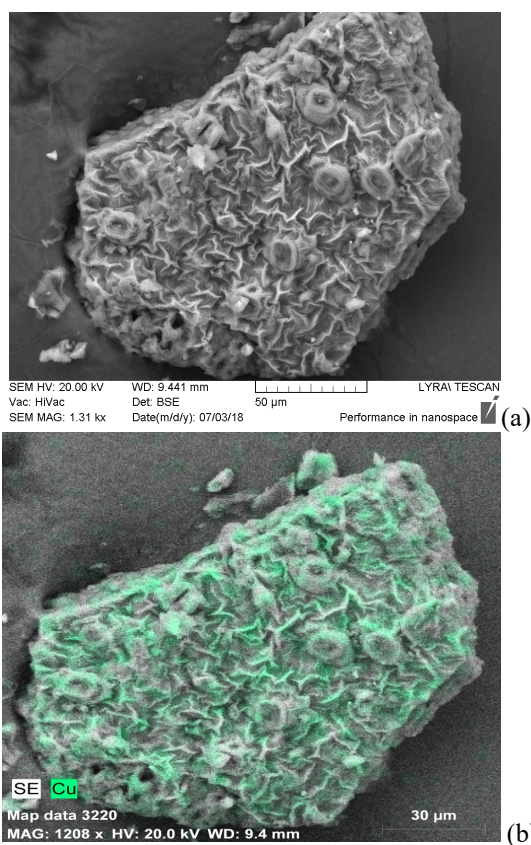


Fig. 3. Scanning electron micrographs of the surface of MO before (a) and after (b) Cu(II) adsorption, respectively

FTIR analysis

FTIR spectroscopy was used to obtain information about the functional groups from the plant material responsible for the metal ion sorption. On Figure 5 the IR spectrum of raw MO and that after Cu(II) adsorption (MOS) are compared. For a better understanding, the bands affected by the

Cu(II) retention are marked by red asterisk. Despite the compositional difference, the spectral picture observed for raw MO resembles those reported for other plant materials [11-13, 24]. Lemon balm, like other herbs, has multicomponent composition. In addition to the common constituents of the plant cells (cellulose, hemicellulose, pectin and lignin) over 100 compounds have been identified in lemon balm [25, 26]. Phytochemical investigations on MO have revealed that the main components are: a large number phenolic acids (more than 15), particularly derivatives of hydroxycinnamic acid; tannins; flavonoids; monoterpene glycosides; sesquiterpenes and essential oils [26]. The rich multicomponent nature of MO determines a complex IR spectroscopic picture, which is characterized by intensive overlapping of a huge number of bands associated with vibrations of the various structure units building its individual constituents (Fig. 4).

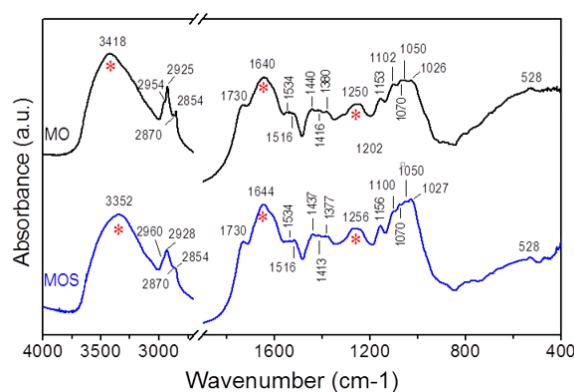


Fig. 4. FTIR spectra of raw MO and after Cu(II) biosorption process (MOS).

The hydroxyl groups from different phenolic structures, COOH groups and water molecules, all involved in hydrogen bonds, give rise to the strong band centered at 3418 cm⁻¹ (O-H stretching vibrations). The presence of methylene, methyl and unconjugated carbonyl groups is doubtless: bands in the regions of 2960-2850 cm⁻¹ (C-H stretching vibrations) and 1440-1380 cm⁻¹ (C-H bending vibrations) and the band at 1730 cm⁻¹ (C=O stretches). The strong absorption at 1640 cm⁻¹ is attributed to the stretching vibrations of C=C double bonds (isolated and conjugated), ring conjugated C=O bonds and C-O bonds in carboxylate groups. The bands at 1534 and 1516 cm⁻¹ can be related to the aromatic ring vibrations and C-O stretching modes in carboxylate groups. The stretching vibrations $\nu(\text{C-O})$ in both phenolic OH and COOH groups plus $\nu(\text{C-O-C})$ stretching vibrations in esters and aromatic ethers are mainly responsible for the band around 1250 cm⁻¹. The spectral picture in the

region of 1150 - 1020 cm^{-1} also has very complex origin: $\nu(\text{C}-\text{O})$ stretching modes in alcoholic C-OH groups, $\nu(\text{C}-\text{O}-\text{C})$ stretching modes in esters and aliphatic ethers, cyclic ring vibrations, aromatic C-H bending and CH_3 bending vibrations. The broad asymmetric absorption observed below 850 cm^{-1} is a result of intensive overlapping of bands associated with bending vibrations of different groups (aromatic C-H, O-H, $=\text{CH}$, C-C rings), skeleton deformations of aromatic and unsaturated structures, etc.

From the spectroscopic analysis it can be concluded that MO offers many oxygen-containing functional groups which are able to interact with the Cu(II) ions. The comparison of the IR spectra of the plant material before and after treatment indicates that the IR spectrum is very little affected by the Cu(II) retention. The overall spectral picture remains almost the same and only a frequency shift of three bands can be surely detected (shift greater than the instrumental resolution). These are: the one at 3423 cm^{-1} which exhibits a large low-frequency shift with 26 cm^{-1} , and the other two bands at 1640 and 1250 cm^{-1} which display a smaller high-frequency shift with 4 and 6 cm^{-1} , respectively. From the interpretation given above it follows that the spectral changes refer mainly to OH (phenolic and carboxylic ones), carbonyl and carboxyl groups. The participation of C-O-C groups from esters and aromatic ethers is not so obvious, but it cannot be fully ignored since the stretching vibrations of these groups contribute to the band at 1256 cm^{-1} as well. The observed band shifting after the copper retention gives indication for a change in the strength of intramolecular interactions of the type O-H, C-O, C=O and C-O-C which could be related with interactions between Cu(II) ions and the oxygen atoms from the functional groups.

It should be mentioned that in the literature the values of the observed band frequency shifts due to metal ion retention, including copper ions, on natural sorbents vary within broad limits, between 3 and 37 cm^{-1} as the largest shifts have been found for the $\nu(\text{OH})$ band [11, 12, 24, 27].

In the literature different mechanisms of metal ions adsorption on herbs including complexation, ion exchange and electrostatic attraction have been discussed [27, 28] Unequivocal interpretation is very difficult, thus the retention of Cu(II) on MO cannot be attributed directly to one of them. Probably, this process is a combination of all possible interactions, pointing to its complex nature.

XPS analysis

XPS is one of the most useful tools for analyzing the adsorption interaction and the type and relative amount of chemical groups on the adsorbent surfaces. The surfaces of the investigated material – before (MO) and after adsorption of Cu(II) ions (MOS) were studied. To elucidate the retention mechanism of Cu(II) onto MO surface, the changes in the C1s, O1s and Cu2p3/2 photoelectron spectra were recorded and are presented in Figure 5 and Table 3.

In order to get an insight into the concentration of the functional groups before and after Cu(II) adsorption, a curve-fitting procedure for carbon C1s peaks was performed as follows. The high resolution C1s photoelectron peaks recorded for the examined samples were split to three components named C1, C2 and C3, respectively and related to different existing bonds on their surfaces. The major C1 peak component (at ≈ 285 eV) is associated to C-C bond; the second C2 peak at ≈ 286.5 eV corresponds to the C-OH, C-O bond, or C-N; and the C3 peak situated at ≈ 288.0 eV corresponds to O-C=O bond.

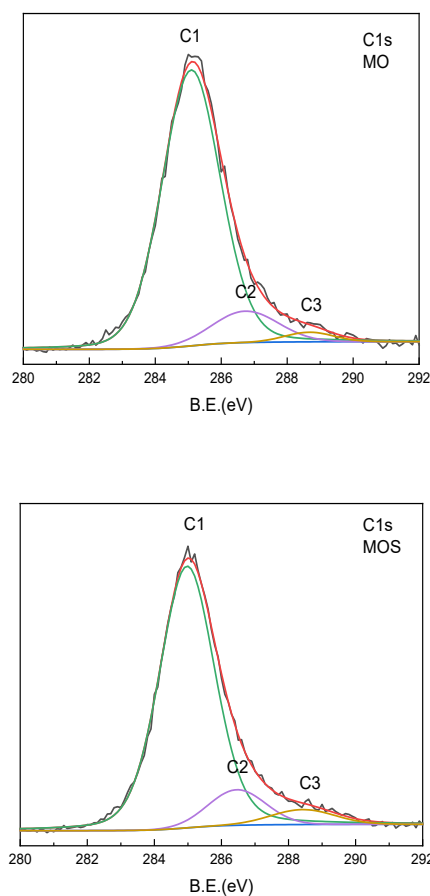


Fig. 5. C1s photoelectron spectra/binding energies (B.E.) of MO and MOS

Table 4. Calculated relative amounts of carbon functional groups present on the surface of MO and MOS

Sample	C1	C2	C3	O1	O2
	C-C, %	C-O-C, C-OH, C-N, %	O-C=O, %	C=O, %	C-O, %
MO	87.1	10.5	2.4	34.6	65.4
MOS	84.2	10.8	5.0	62.3	37.7

% from total carbon and oxygen

These peaks can be assigned to C atoms in the form of C–C, C–O (alcoholic or ether), O–C–O (ether) and O–C=O (carboxylate or ester groups), respectively [11, 29]. The O1s spectra (figures not presented) show two components at around 532.5 eV and 533.5 eV. Both components can be assigned to the existence of functional groups such as C=O and C-O/C-OH, respectively, but not to Cu-O.

On the other hand, the XPS results show that the Cu2p_{3/2} peak has binding energy at around 933.5 eV accompanied by the satellite peak at around 943 eV, typical for Cu(II). The relative contents of C-C, C-OH or C-O/C-N and C=O functional groups changed after Cu(II) adsorption which is in accordance with the FTIR analysis. The relative amount of C-C and C=O increase after copper adsorption while the relative amount of C-O, C-OH, C-N decreases (Table 4) pointing out that the mechanism of copper ions retention on MO has a multiplex character. The contribution of XPS results to the above discussion additionally reveals the complex nature of the investigated biosorption process between Cu(II) and MO, which proved to be a combination of surface complexation, ion exchange and electrostatic attraction, in accordance with literature data [11-13].

CONCLUSIONS

Biomaterial based on lemon balm (*Melissa officinalis* L.) was evaluated as a sorbent for Cu(II) removal from aqueous media. The influence of the acidity of the initial metal ion solutions on its adsorption was investigated, and the optimal pH value was found to be about 4. The adsorption equilibrium was established within 10 min. The adsorption isotherm exhibits mainly Langmuir behaviour which assumes that the uptake of copper ions occurs on a homogeneous surface by monolayer adsorption. Desorption studies demonstrate that 1M HNO₃ and 0.1 M EDTA could be used as eluting agents. The maximum adsorption capacity was found to be 59.95 mg g⁻¹, showing that MO could be used as an effective biosorbent for the removal of copper ions.

The sorption mechanism was further investigated by means of FTIR and XPS. It was established that the retention of Cu(II) ions on the surface of raw MO

and its biomass is a result of interactions between these ions and the OH groups from the phenolic structures and COOH groups, but the participation of esters and aromatic ether groups cannot be ignored. The adsorption proved to be a multiplex process that involves surface complexation, ion exchange and electrostatic attraction.

Acknowledgements: The authors thank to Assoc. Prof. Ivalina Avramova for her help by elucidation the XRS-results. This work is supported by the Bulgarian Ministry of Education and Science under the National Research Programme “Healthy Foods for a Strong Bio-Economy and Quality of Life” approved by DCM # 577 / 17.08.2018 and the National Roadmap for Research Infrastructure (2017-2023): Research Infrastructure Energy Storage and Hydrogen Energetics ESHER, grant agreement D01-161/28.07.22.

REFERENCES

1. I. Ugulu, *Appl. Spectrosc. Rev.*, **50**, 113 (2015).
2. M. Aryal, *Rev. Chem. Eng.*, **37**, 715 (2021).
3. H. Zhang, X. Hu, H. Lu, *Water Sci. Technol.*, **76**, 859 (2017).
4. A. A. Redha, *Arab. J. Basic Appl. Sci.*, **27**, 183 (2020).
5. K. Chojnacka, M. Mikulewicz, *TrAC – Trend. Anal. Chem.*, **116**, 254 (2019).
6. L. Ivanova, P. Vassileva, G. Gencheva, A. Detcheva, *J. Environ. Prot. Ecol.*, **21**, 37 (2020).
7. P. S. Vassileva, L. P. Ivanova, A. K. Detcheva, *Bulg. Chem. Commun.*, **54**(A), 19 (2022)
8. S. Miraj, M. Rafiean Kopae, S. Kiani, *J. Evid. Based Complementary Altern. Med.*, **22**, 385 (2017)
9. S. A. Aransiola, U. J. J. Ijah, O. P. Abioye, J. D. Bala, *Int. J. Environ. Sci. Technol.*, **20**, 1823 (2023)
10. V. D. Zheljazkov, E. A. Jeliakova, N. Kovacheva, A. Dzhurmanski, *Environ. Exp. Bot.*, **64**, 207 (2008)
11. J.-C. Zheng, H.-M. Feng, M. H.-W. Lam, P. K.-S. Lam, Y.-W. Ding, H.-Q. Yu, *J. Hazard. Mater.*, **171**, 780 (2009).
12. W. S. Wan Ngah, M. A. K. M. Hanafiah, *J. Environ. Sci.*, **20**, 1168 (2008).
13. X. Liu, Z.-Q. Chen, B. Han, C.-L. Su, Q. Han, W.-Z. Chen, *Ecotox. Environ. Safe.*, **150**, 251 (2018).
14. G. Gentsheva, P. Vassileva, N. Marinkov, C. Tzvetkova, D. Kovacheva, *C. R. Acad. Bulg. Sci.*, **73**, 1229 (2020).

15. A. O. Dada, A. P. Olalekan, A. M. Olatunya, O. Dada, *IOSR J. Appl. Chem.*, **3**, 38 (2012).
16. P. Vassileva, D. Voykova, I. Uzunov, S. Uzunova, *C. R. Acad. Bulg. Sci.*, **71**, 1192 (2018).
17. C. Liu, H. H. Ngo, W. Guo, K.-L. Tung, *Bioresour. Technol.*, **119**, 349 (2012)
18. M. N. Stanković, N. S. Krstić, J. Z. Mitrović, S. M. Najdanović, M. M. Petrović, D. V. Bojić, V. D. Dimitrijević, A. L. Bojić, *New J. Chem.*, **40**, 2126 (2016)
19. Z.-Y. Yao, J.-H. Qi, L.-H. Wang, *J. Hazard. Mater.*, **174**, 137 (2010)
20. S.-Y. Lee, H.-J. Choi, *J. Environ. Manage.*, **209**, 382 (2018)
21. L. Ivanova, P. Vassileva, A. Detcheva, *Mater. Today: Proc.*, **61**, 1237 (2022)
22. M. A. Darweesh, M. Y. Elgendy, M. I. Ayad, A. M. M. Ahmed, N. M. Kamel Elsayed, W. A. Hammad, *S. Afr. J. Chem. Eng.*, **40**, 10 (2022)
23. H. M. Adeel, B. Parveen, N. Rasool, M. Riaz, K. G. Ali, Y. Gull, M. Noreen, M. Asghar, *Int. J. Chem. Biochem. Sci.*, **4**, 38 (2013)
24. X. Zhu, H. Yu, H. Jia, Q. Wu, J. Liu, X. Li, *Anal. Methods*, **5**, 4460 (2013).
25. C. G. Boeriu, D. Bravo, R. J. A. Gosselink, J. E. G. van Dam, *Ind. Crop. Prod.*, **20**, 205 (2004);
26. A. Shakeri, A. Sahebkar, B. Javadi, J. Ethnopharmacol., 188, 204 (2016).
27. M. Petrović, T. Šoštarić, M. Stojanović, J. Petrović, M. Mihajlović, A. Čosović, S. Stanković, *Ecol. Eng.*, **99**, 83 (2017).
28. M. Khormaei, B. Nasernejad, M. Edrisi, T. Eslamzadeh, *J. Hazard. Mater.*, **149**, 269 (2007).
29. G. Vázquez, M. Calvo, M. S. Freire, J. González-Alvarez, G. Antorrena, *J. Hazard. Mater.*, **172**, 1402 (2009).